

Communication

The ZVS Class E/F₃ Inverter Using Piezoelectric Transformers for Energy Extraction

Ratil H. Ashique¹, M. Saad Bin Arif^{2,*}, Abdul Rauf Bhatti³, Ahmed Al Mansur¹, Md. Hasan Maruf¹
and ASM Shihavuddin¹

¹ Department of Electrical and Electronic Engineering, Green University of Bangladesh, Dhaka 1207, Bangladesh

² Department of Electrical and Electronic Engineering, Aligarh Muslim University, Aligarh 202002, Uttar Pradesh, India

³ Department of Electrical Engineering and Technology, Government College University Faisalabad, Faisalabad 38000, Pakistan

* Correspondence: saad.ee@amu.ac.in

Abstract: Enhanced class E inverters (EF_n or E/F_n) reduce the high peak switch voltage that is prevalent in class E inverters. Additionally, their stability and load regulation capabilities are improved as compared to class E inverters. This paper proposes an enhanced class E inverter (E/F₃) with a piezoelectric transformer (PT) replacing the auxiliary resonant networks. This class E/F₃ inverter is designed by adding a tuned auxiliary LC network at the third harmonic of the switching frequency to the class E inverter. Both the primary and auxiliary resonant networks are realized using a piezoelectric transformer (PT). The converter is simulated in LTspice and an experimental prototype is built and tested. It is found that the experimental results concur with the simulation results, with a measured efficiency of 90%. Thus, the theoretical design is verified and the concept of energy extraction is achieved.

Keywords: class E; class E/F₃; ZVS



Citation: Ashique, R.H.; Arif, M.S.B.; Bhatti, A.R.; Al Mansur, A.; Maruf, M.H.; Shihavuddin, A. The ZVS Class E/F₃ Inverter Using Piezoelectric Transformers for Energy Extraction. *Electronics* **2023**, *12*, 2118. <https://doi.org/10.3390/electronics12092118>

Academic Editor: Ahmed Abu-Siada

Received: 30 December 2022

Revised: 10 March 2023

Accepted: 16 March 2023

Published: 6 May 2023



Copyright: © 2023 by the authors. Licensee MDPI, Basel, Switzerland. This article is an open access article distributed under the terms and conditions of the Creative Commons Attribution (CC BY) license (<https://creativecommons.org/licenses/by/4.0/>).

1. Introduction

The compact architecture of class E inverters, which has a low component count and a simultaneous high power transmission capability, is largely responsible for their popularity. Additionally, if combined with zero voltage switching (ZVS) or zero derivative voltage switching (ZVDS) approaches, they can function at very high switching frequencies with excellent efficiency. The ZVS/ZVDS class E inverters' analyses and modeling have been thoroughly documented in the literature [1–3]. This architecture does have one significant drawback, though. This is seriously concerning, because the peak switch voltage is so large (3.5 to 5 times, depending on the duty ratio) [4–8]. The upgraded class E configurations are suggested, among other things, to address this problem, and the LC networks are tuned at the *n*th harmonic of the switching frequency [9–18]. In this paper, a class E/F₃ inverter is designed. The inverter's topology is shown in Figure 1a. A piezoelectric transformer (PT-T1PP0361) is used for energy extraction in the primary and auxiliary resonant networks. This PT is shown in Figure 1b, along with its mason equivalent circuit being demonstrated in Figure 1c. In Figure 1a, the inverter has primary and secondary resonant networks tuned at different resonant frequencies. In this design, either the primary or secondary resonant network is replaced by the PT, or the PT is used to realize the other network using conventional magnetic components. The experimental prototype is constructed and put through testing, while the inverter is simulated in LTSPICE utilizing a PT emulation circuit. The following sections provide details on the testing's design and outcomes. In Section 2, the circuit configuration and modes of operation are described. In Section 3, the circuit

design is explained. In Section 4, the simulation and experimental verification process is described. Section 5 concludes the paper.

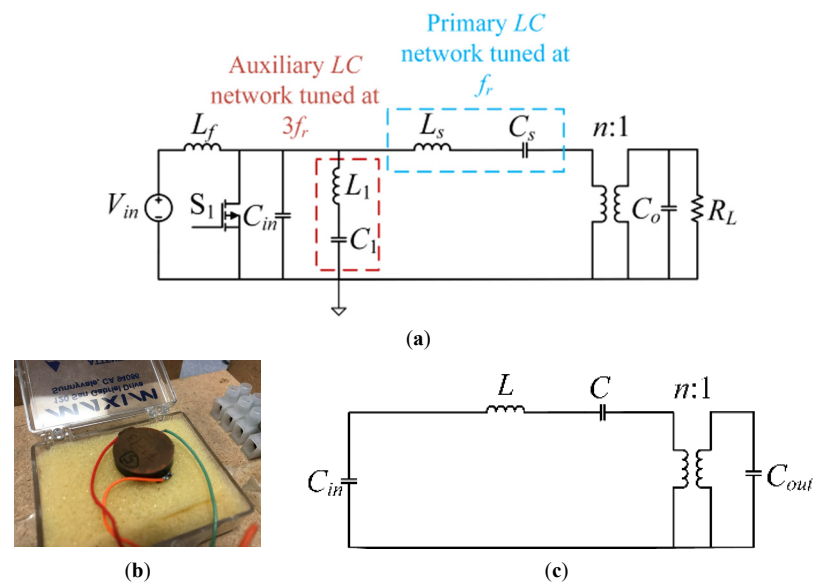


Figure 1. (a) The class E/F3 topology with primary and auxiliary resonant networks tuned at f_r and $3f_r$, respectively. (b) The radial mode PT (T1PP0361). (c) The PT mason equivalent circuit.

2. The Circuit Configuration and Modes of Operation

In Figure 1a, the inductance L_s and capacitance C_s make up the primary resonant tank of the class E/F₃ inverter, which resonates at a resonant frequency (f_r) in accordance with a quality factor (Q). The input inductance (L_f) is designed to deliver an extremely low ripple current while maintaining a steady DC current. The input capacitance C_{in} absorbs the drain-to-source (non-linear) capacitance (C_{ds}) of the switch. The auxiliary resonant branch consists of the auxiliary resonant inductance (L_1) and capacitance (C_1). The primary resonant frequency is f_r , and the auxiliary resonant frequency is $3f_r$. The primary resonant frequency f_r and the switching frequency f_s are both chosen to be equal, or the f_s is slightly higher than the f_r . To accomplish the ZVS operation, the switch S_1 is run at its optimal duty ratio D_{opt} . The switching pattern is depicted as follows.

$$\text{Switch} = \begin{cases} \text{Turned ON, } 0 \leq \theta < 2\pi D \\ \text{Turned OFF, } 2\pi D \leq \theta < 2\pi \end{cases} \quad (1)$$

When the switch S_1 is ON in mode 1, the voltage across the capacitor C_{in} is forced to zero. The L_f is charged as the input current (I_{in}) passes through S_1 . The resonant current flows through the switch in the resonant tank, transferring the stored energy from the C_s to the L_s and completing one half of the resonant cycle. At the conclusion of this cycle, the energy transfer is completed and the current starts to decline. When S_1 opens at $\theta = 2\pi D$ in mode 2, the I_{in} charges the input capacitor C_{in} , which eventually achieves the peak switch voltage ($V_{S1,peak}$), before being discharged through the primary resonant tank. Due to the inductive nature of the load network in mode 2, the output current (I_{out}) lags the input voltage to the resonant tank (V_{S1}) in mode 2. This ensures that the ZVS is operating for the designed inverter. On that note, the following conditions must be met to achieve ZVS or ZVDS,

$$V_{S1}(2\pi) = 0 \text{ and } \frac{d}{d\theta} V_{S1}(2\pi) = 0 \quad (2)$$

In Figure 1b, the PT mason equivalent circuit replaces the primary or the secondary resonant tank in the class E/F₃ resonant inverter.

3. Circuit Design

In this section, the circuit components are designed [7,8] according to the specifications that are stated in Table 1. As mentioned earlier, the primary and auxiliary resonant tank is replaced by the PT. The PT characteristic component values are measured using a Bode 100 Network Analyzer. The measured parameters are stated in Table 2.

Table 1. Design specifications.

Parameters	Symbols	Values
Input voltage	V_{in}	10 V
Primary resonant frequency	f_r	26.67 kHz
Auxiliary resonant frequency	$3f_r$	80 kHz
Capacitance ratio	$k (C_1/C_{in})$	10
Quality factor of the conventional resonant tank	Q_{aux}	0.707

Table 2. Characteristic component values of PT.

Parameter	Symbol	Value
Series resistance	R_{PT}	8.69 Ω
Resonant inductor	L_S	4.86 mH
Resonant capacitor	C_S	0.814 nF
Input capacitor	C_{in}	2.53 nF
Output capacitor	C_o	4.58 nF
Turns ratio	$n:1$	1:0.45
Quality factor of the PT	Q_{PT}	281.30

As can be calculated from Table 2, the PT resonant frequency (f_{r-PT}) is

$$f_{r-PT} = \frac{1}{2\pi\sqrt{LC}} = \frac{1}{2\pi\sqrt{4.86 \times 10^{-3} \times 0.814 \times 10^{-9}}} \approx 80 \text{ kHz} \quad (3)$$

An input inductor $L_f = 100 \mu\text{H}$ is selected for both designs involving the PT, as the primary or auxiliary resonant network.

A. The PT as Primary Resonant Tank

In this subsection, the inverter is designed while the primary resonant tank is replaced by a PT. In Figure 2, the circuit diagram with the PT mason equivalent circuit is shown. In this case, as can be derived from Table 2, $L_s = L_{PT} = 4.86 \text{ mH}$, $C_s = C_{PT} = 0.814 \text{ nF}$, $n \approx 2.22$, $C_{in} = C_{in-PT} = 2.53 \text{ nF}$, and $C_o = C_{out-PT} = 4.58 \text{ nF}$. The $L_{of}C_{of}$ filter is designed with a cutoff frequency of $f_c = 120 \text{ kHz}$. Alternatively, without the $L_{of}C_{of}$ filter, a large output capacitor, $C_{of} = 330 \mu\text{H}$, can be used to reduce the high frequency harmonics, as shown in Figure 2b. As the PT replaces the primary resonant tank, the primary resonant frequency f_r is 80 kHz. The auxiliary circuit has to resonate at $f_{raux} = 3f_r$. The components L_1 and C_1 are selected for $Q = 0.707$ from Table 1 and for $R_L = 100 \Omega$.

$$L_1 = \frac{Q \times R_L}{\omega} = \frac{0.707 \times 100}{2\pi \times 240 \times 10^3} \approx 46.90 \mu\text{H} \quad (4)$$

$$C_1 = \frac{1}{4\pi^2 L_1 f_{raux}^2} = \frac{1}{4\pi^2 \times 46.90 \times 10^{-6} \times (3 \times 80 \times 10^3)^2} \approx 9.38 \text{ nF} \quad (5)$$

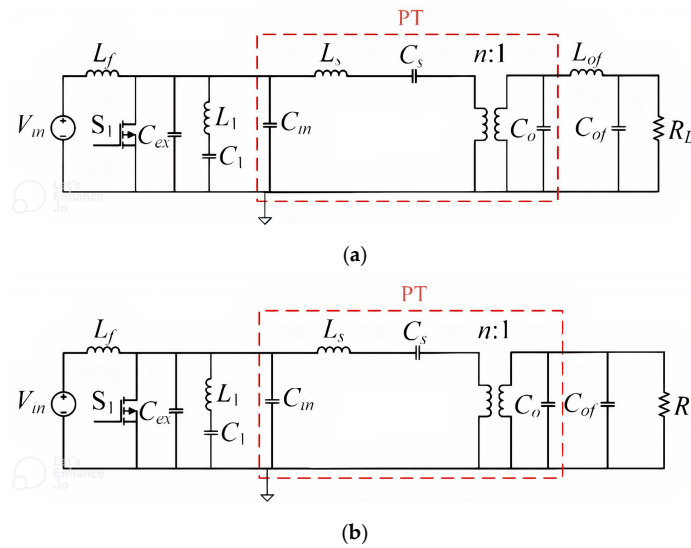


Figure 2. PT as primary resonant tank, (a) with an output LC filter, and (b) with output filter capacitor (C_{of}).

The input capacitance can be calculated from [12] by using the k from Table 1.

$$\omega R_{L,opt} C_{in} = \frac{0.6428k + 0.3598}{k + 0.0875} \Rightarrow C_{in} = \frac{0.6428 \times 10 + 0.3598}{2\pi \times 26670 \times 100 \times (10 + 0.0875)} = 40.15 \text{ nF} \tag{6}$$

As $C_{in-PT} = 2.53 \text{ nF}$, an external input capacitance $C_{ex} = C_{in} - C_{in-PT} = (40.15 - 2.53) \text{ nF} = 37.62 \text{ nF}$ has to be added. Practically, $C_{ex} \approx 47 \text{ nF}$ is selected with consideration to its availability. The circuit parameters are stated in Table 3.

B. The PT as Auxiliary Resonant Tank

Table 3. The circuit parameters with PT as primary resonant tank.

Parameter		Values
PT input capacitance	C_{in}	2.53 nF
External input capacitance	C_{ex}	47 nF
PT output capacitance	C_o	4.70 nF
PT transformer ratio	n	≈ 2.22
Load resistance	R_L	100 Ω
Primary resonant inductance	L_s	4.77 mH
Primary resonant capacitance	C_s	814 pF
Auxiliary resonant inductance	L_1	46.90 μH
Auxiliary resonant capacitance	C_1	9.10 nF
Output filter inductor	L_{of}	200 μH
Output filter capacitance	C_{of}	100 nF

In Figure 3, the circuit diagram, with the PT replacing the auxiliary resonant network, is shown. In this case, as can be derived from Table 2, $L_1 = L_{PT} = 4.86 \text{ mH}$, $C_1 = C_{PT} = 0.814 \text{ nF}$, $n \approx 2.22$, and $C_{in} = C_{in-PT} = 2.53 \text{ nF}$. For the structure of the PT, the $C_{out-pri}$ comes in parallel to the C_1 . This is due to the PT output capacitance (C_{out-PT}) being reflected to the primary side and can be computed as:

$$C_{out-pri} = C_{out-PT} \times n^2 = 4.58 \times (2.22)^2 \text{ nF} = 22.57 \text{ nF} \tag{7}$$

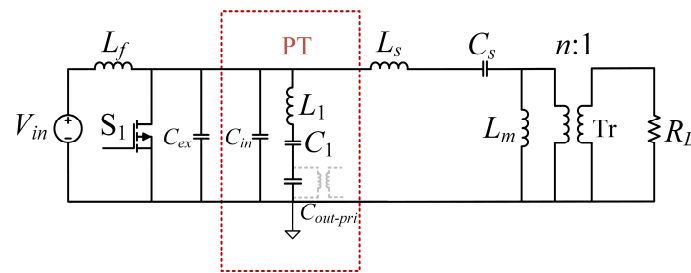


Figure 3. The class E/F₃ topology with PT as auxiliary resonant tank and magnetic transformer.

In (6), the required C_{in} is calculated. Hence, an external input capacitance, $C_{ex} \approx 47$ nF, is added to the required design. The magnetic transformer (Tr) has a magnetic inductance of $L_m = 18$ μ H. The circuit parameters are stated in Table 4.

Table 4. The circuit parameters with PT as auxiliary resonant tank.

Parameter		Values
PT input capacitance	C_{in-PT}	2.53 nF
External input capacitance	C_{ex}	47 nF
PT output capacitance	C_{out-PT}	4.57 nF
Transformer ratio	$n:1$	2:1
Load resistance	R_L	100 Ω
PT auxiliary resonant inductance	L_1	4.86 mH
PT auxiliary resonant capacitance	C_1	814 pF
PT output capacitance	$C_{out-pri}$ ($n^2 * C_{out-PT}$)	18.28 nF
Equivalent capacitance in the auxiliary branch	$C_{eq} = C_1 C_{out-pri}$	778 pF
Primary resonant inductance	L_s	300 μ H
Primary resonant capacitance	C_s	124 nF

4. Simulation and Experimental Verification

The class E/F₃ inverter with the integrated PT is simulated in an LTSPICE simulation platform and prototypes are built. In Figure 4, the LTSPICE simulation circuit is shown. In this configuration, the PT emulator (i.e., the mason equivalent) replaces the primary resonant tank. The component design is presented in the previous section and utilizes a PT as the primary or auxiliary resonant network. In the rest of this section, the results for the simulation and experimentation of the designed inverter are presented and described. The experimental setup is shown in Figure 5.

A. The PT as Primary Resonant Tank

In Figure 5, the LTSPICE simulation circuit is shown. In this configuration, the PT emulator (i.e., the mason equivalent) replaces the primary resonant tank.

In Figure 6a, the switch voltage from the LTSPICE simulation is demonstrated. As can be seen, the peak switch voltage is 34 V. From Figure 6b, it is obvious that the output voltage (V_{out}) is smooth and contains less harmonics. However, the reverse diode’s conduction shows that the inverter is not performing at its best. The inverter’s output power is determined as follows:

$$P_{out,sim} = \frac{V_{rms}^2}{R_L} \approx \frac{(18 \times 0.707)^2}{100} = 1.62 \text{ W} \tag{8}$$

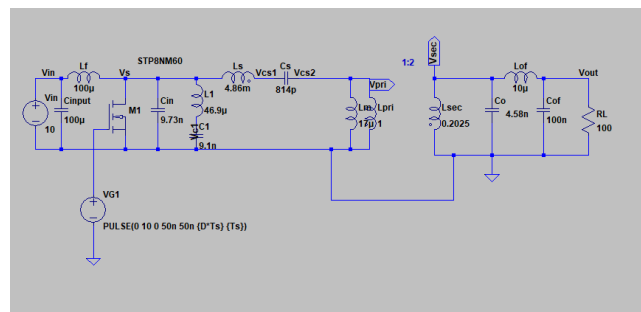


Figure 4. Simulation circuit: the class E/F₃ topology with PT as primary resonant tank.

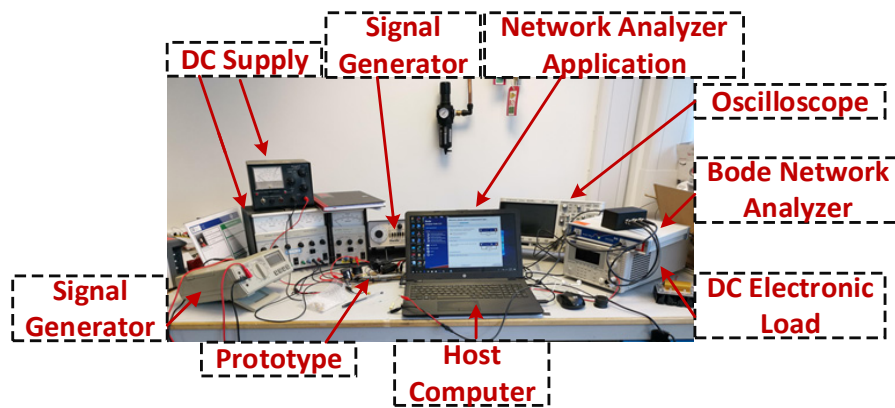


Figure 5. Experimental setup.

The experimental findings are shown in Figure 7. As can be seen, the switch’s reverse diode (S_1) conducts for a brief length of time, achieving the ZVS/ZDS in the sub-optimal zone. This output power is determined as follows:

$$P_{out,exp} = \frac{V_{rms}^2}{R_L} \approx \frac{(20 \times 0.707)^2}{100} = 1.99 \text{ W} \tag{9}$$

The high frequency harmonics in the V_{out} can be decreased using an LC low pass filter or an output capacitor, as shown in Figure 7b,c. Additionally, it is clear that the simulation and experimental results closely support the theoretical design. Table 5 compiles the findings to show how comparable they are.

B. The PT as Auxiliary Resonant Tank

Table 5. The simulation and experimental prototype results.

Parameter	Simulation	Experimental
PT as primary resonant tank		
V_{out}	18 V	20.9 V
$V_{S1,peak}$	34 V	36.1 V
$V_{C1,peak}$	48 V	53.2 V
PT as auxiliary resonant tank		
V_{out}	2.6 V	3.2 V
$V_{S1,peak}$	70 V	45.9 V

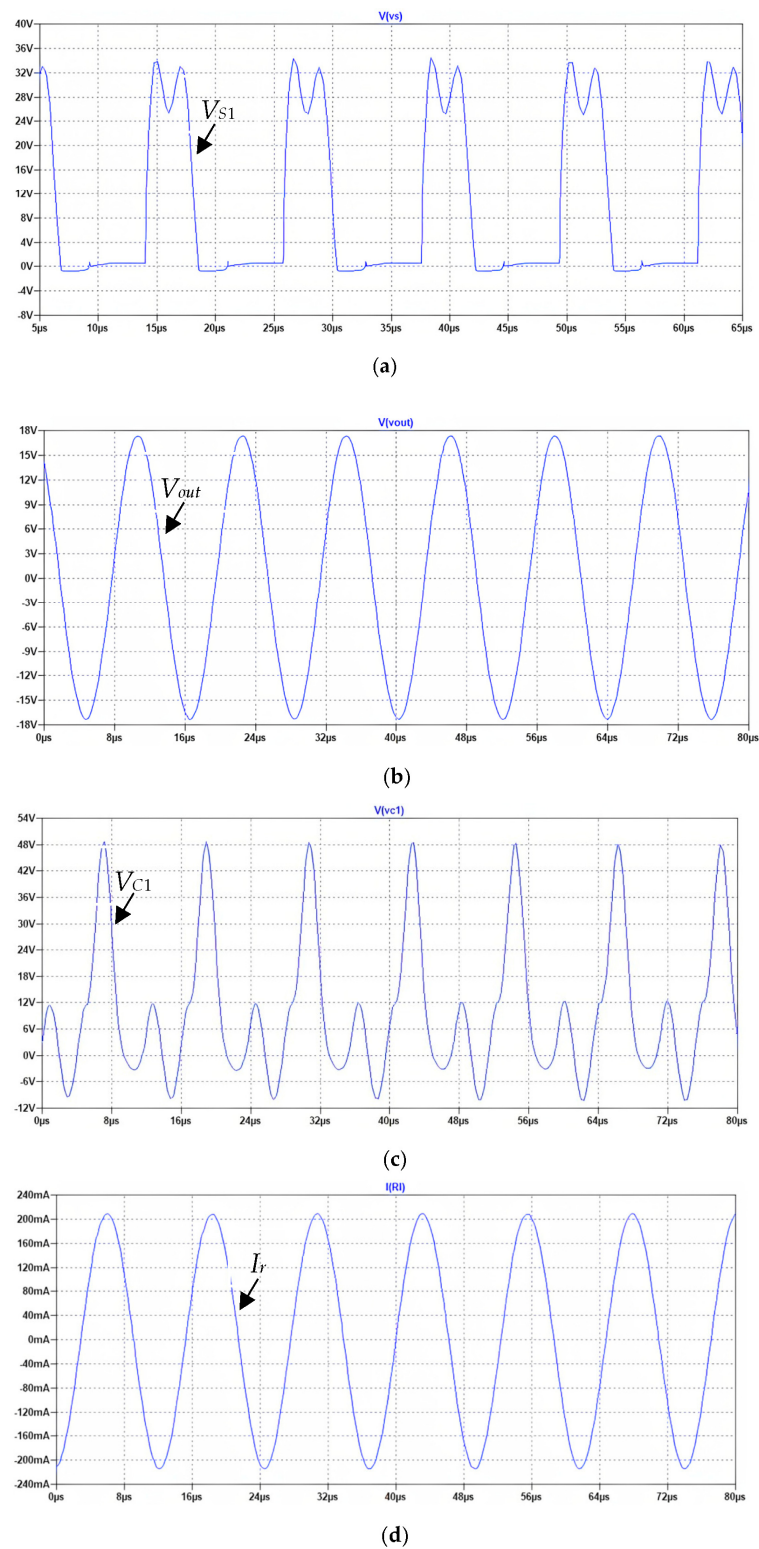
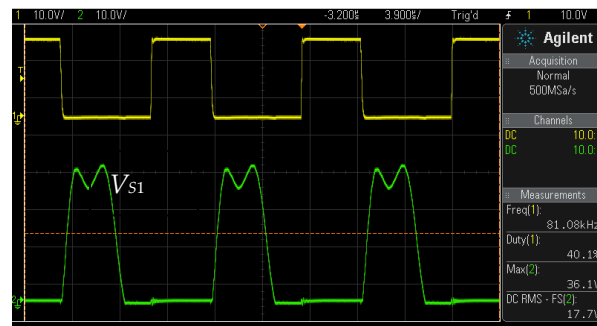
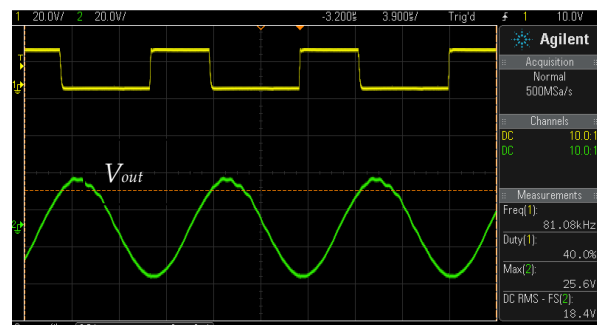


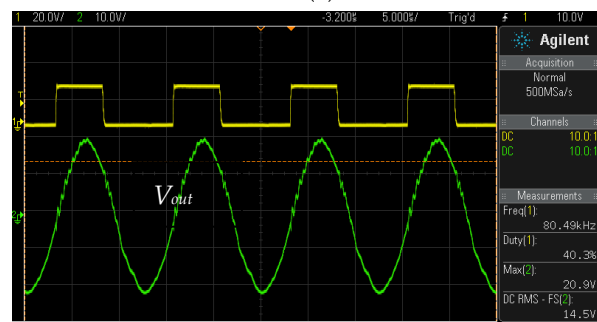
Figure 6. Simulation results: the class E/F3 topology with PT as auxiliary resonant tank. (a) The switch voltage, (b) the output voltage, V_{out} (c) the auxiliary resonant capacitor voltage, V_{C1} , and (d) the primary resonant current, I_r .



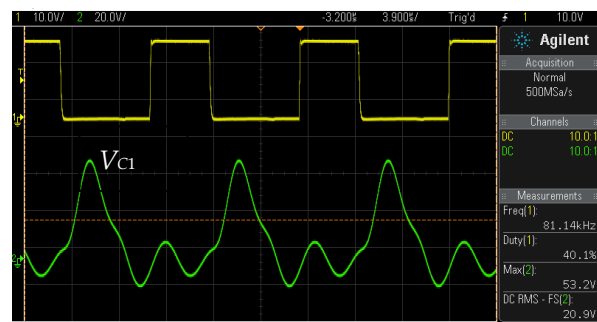
(a)



(b)



(c)



(d)

Figure 7. Experimental results for class E/ F_3 topology with piezoelectric transformer as primary resonant tank. (a) The switch voltage, V_{S1} , (b) the output voltage with LC output filter, V_{out} , (c) the output voltage with output filter capacitance, V_{out} , and (d) the auxiliary resonant capacitor voltage, V_{C1} .

In Figure 8, the LTSPICE simulation circuit is shown for the PT that replaces the conventional auxiliary resonant network. In this configuration, the PT emulator (i.e., the mason equivalent) is used for simulation purposes.

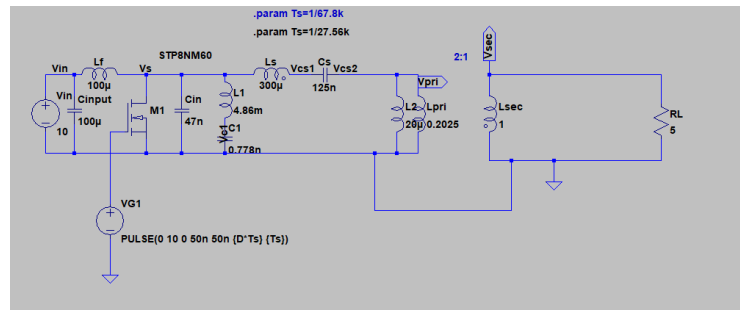
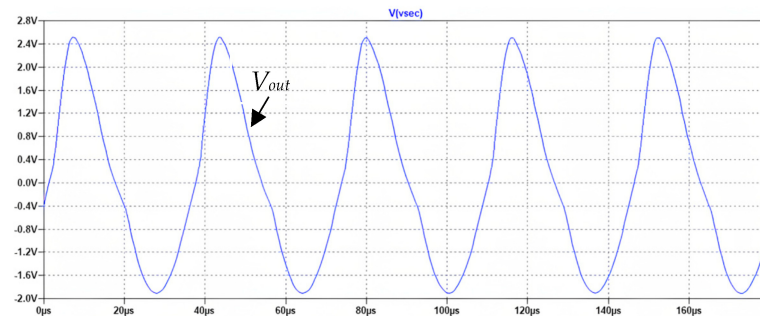
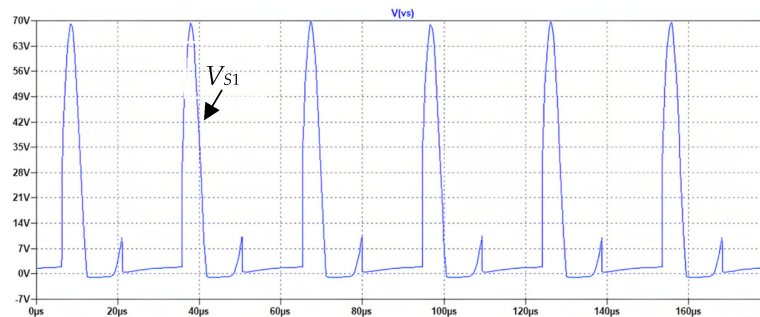


Figure 8. Simulation circuit: the class E/F3 topology with PT as auxiliary resonant tank.

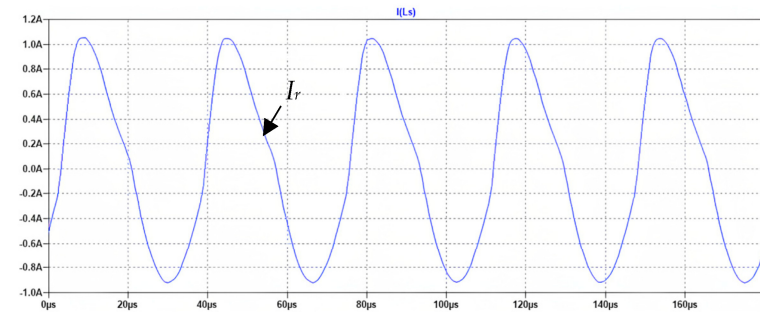
The simulation results are shown in Figure 9. The ZVS is attained, as seen by the switch voltage waveform in Figure 9b. However, the reverse diode’s conduction also suggests that the converter is not performing at its best.



(a)



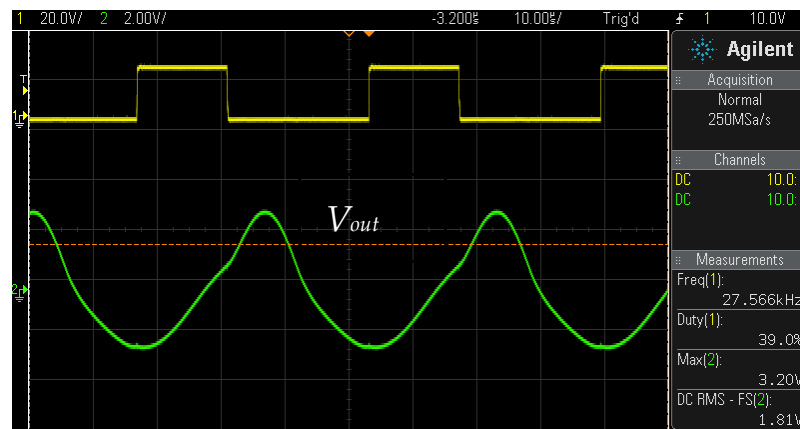
(b)



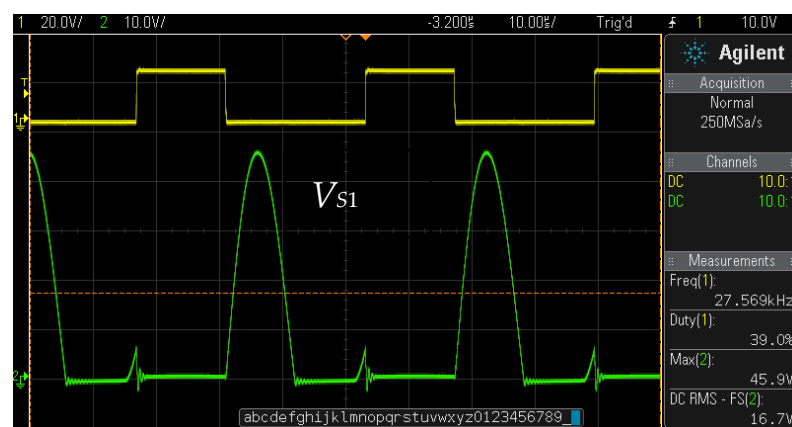
(c)

Figure 9. Simulation results for class E/F3 topology with PT as auxiliary resonant tank. (a) The output voltage, V_{out} , (b) the switch voltage, V_{S1} , and (c) The primary resonant current, I_r .

The experimental findings for the PT working as an auxiliary resonant tank are shown in Figure 10. It is clear from Figure 10a that a higher harmonic content dominates the output voltage (V_{out}). To get rid of the higher frequency harmonics, a 100 kHz output low pass filter can be used. Additionally, the ZVS is attained in the sub-optimal region, as seen in Figures 9b and 10b. It should be noticed that the peak switch voltage ($V_{S1,peak}$) is still high, despite employing the auxiliary network (i.e., the PT). By increasing the capacitance ratio k , this high switch peak voltage can be reduced. However, the latter necessitates the use of a different PT, which is not executed in this work because of the non-availability of the required PT. Nevertheless, the idea of utilizing a PT for the energy extraction in a class E/F3 inverter is confirmed. In Figure 11, the power versus the efficiency (η) curve is shown. The efficiency is measured under the specified conditions, as described in Table 1. As observed, the converter operates at approximately 90%, while the output power (P_{out}) is 5 W or lower. Overall, the simulation and experimental results are shown in Table 5. It can be observed that the results are quite consistent with one another and conform to the theoretical design. The slight differences in the results are due to the deviations of the parametric values of the PT equivalent circuit at a high frequency.



(a)



(b)

Figure 10. Experimental results for class E/F₃ topology with PT as primary resonant tank. (a) The output voltage, V_{out} , and (b) the switch voltage, V_{S1} .

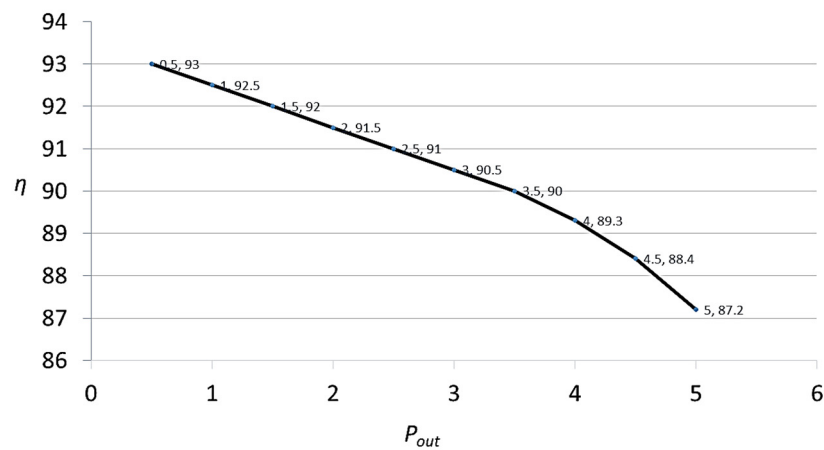


Figure 11. The output power (P_{out}) versus measured efficiency (η).

5. Conclusions

In this paper, the primary or auxiliary resonant tank is replaced with a PT in a class E/ F_3 inverter. According to the circuit analysis, this inverter can be used in ZVS mode while the PT replaces the traditional resonant tanks. The inverter is simulated in LTspice and an experimental prototype of the inverter is tested. The simulation and experimental results are consistent with one another, indicating the validity of the theoretical design. Additionally, by raising the value of k , the inverter's peak switch voltage in the class E/ F_3 can be further reduced, which remains a future scope for this work. A compact and low-power inverter can be realized by replacing its traditional magnetic components with a PT. This concept is also applicable for other enhanced class E inverters. However, there are opportunities for further investigation into this topic.

Author Contributions: Conceptualization, R.H.A. and M.H.M.; methodology, R.H.A., M.S.B.A. and A.S.; validation, R.H.A., A.S. and M.H.M.; formal analysis, A.S.; investigation, R.H.A. and M.H.M.; resources, R.H.A.; data curation, R.H.A. and A.A.M.; writing—original, R.H.A., A.R.B. and A.S.; writing—review and editing, R.H.A. and M.S.B.A.; visualization, R.H.A. and M.H.M.; supervision, R.H.A. All authors have read and agreed to the published version of the manuscript.

Funding: This research received no external funding.

Conflicts of Interest: The authors declare no conflict of interest.

Nomenclature

f_s	Switching frequency
f_r	Resonant frequency
V_{in}	Input voltage
V_{out}	Output voltage
V_{S1}	Switch voltage
I_{in}	Input current
I_{out}	Output current
P_{in}	Input power
P_{out}	Output power
L_s	Primary inductance
C_s	Primary capacitance
L_1	Auxiliary inductance
C_1	Auxiliary capacitance
C_r	Resonant capacitance

C_{out}	Output capacitance
R_L	Load resistance
k	Capacitance ratio
C_{in-PT}	PT equivalent input capacitance
C_{out-PT}	PT equivalent output capacitance
ZVS	Zero Voltage Switching
ZVDS	Zero Voltage Derivative Switching
E/F ₃	Class E/F ₃ Inverter

References

- Huang, J.; Zhang, X.; Li, Y.; Li, Q. A novel ZVS class E/F₃ inverter with piezoelectric transformer for energy harvesting. *IEEE Trans. Ind. Electron.* **2021**, *68*, 400–408. [[CrossRef](#)]
- Islam, M.M.; Islam, M.A.; Faruque, M.R.I. ZVS Class E/F₃ Inverter Using Piezoelectric Transformer for Wireless Power Transfer. *IEEE Trans. Circuits Syst. II Express Briefs* **2021**, *68*, 1421–1425. [[CrossRef](#)]
- Lin, H.; Zhu, J.; Jiao, J.; He, X. Design and implementation of a ZVS class E/F₃ inverter with piezoelectric transformer for wireless power transfer. *IEEE Trans. Ind. Electron.* **2020**, *67*, 1182–1192. [[CrossRef](#)]
- Hayati, M.; Lotfi, A.; Kazimierczuk, M.K.; Sekiya, H. Analysis and Design of Class-E Power Amplifier With MOSFET Parasitic Linear and Nonlinear Capacitances at Any Duty Ratio. *IEEE Trans. Power Electron.* **2013**, *28*, 5222–5232. [[CrossRef](#)]
- Kessler, D.J.; Kazimierczuk, M.K. Power losses and efficiency of class-E power amplifier at any duty ratio. *IEEE Trans. Circuits Syst. I Regul. Pap.* **2004**, *51*, 1675–1689. [[CrossRef](#)]
- Shigeno, A.; Shimizu, T.; Koizumi, H. Current-source parallel resonant class E inverter with low peak switch current. In Proceedings of the IECON 2017—43rd Annual Conference of the IEEE Industrial Electronics Society, Beijing, China, 29 October–1 November 2017; pp. 5330–5335.
- Kaczmarczyk, Z. High-Efficiency Class E, EF₂, and E/F₃ Inverters. *IEEE Trans. Ind. Electron.* **2006**, *53*, 1584–1593. [[CrossRef](#)]
- Ayachit, A.; Corti, F.; Reatti, A.; Kazimierczuk, M. Zero-Voltage Switching Operation of Transformer Class-E Inverter at Any Coupling Coefficient. *IEEE Trans. Ind. Electron.* **2018**, *66*, 1809–1919. [[CrossRef](#)]
- Kaczmarczyk, Z.; Jurczak, W. A Push–Pull Class-E Inverter With Improved Efficiency. *IEEE Trans. Ind. Electron.* **2008**, *55*, 1871–1874. [[CrossRef](#)]
- Kazimierczuk, M.K.; Jozwik, J. DC/DC converter with class E zero-voltage-switching inverter and class E zero-current-switching rectifier. *IEEE Trans. Circuits Syst.* **1989**, *36*, 1485–1488. [[CrossRef](#)]
- Li, Y.; Sue, S. Exactly analysis of ZVS behavior for class E inverter with resonant components varying. In Proceedings of the 2011 6th IEEE Conference on Industrial Electronics and Applications, Beijing, China, 21–23 June 2011; pp. 1245–1250.
- Kee, S.D.; Aoki, I.; Hajimiri, A.; Rutledge, D. The class-E/F family of ZVS switching amplifiers. *IEEE Trans. Microw. Theory Tech.* **2003**, *51*, 1677–1690. [[CrossRef](#)]
- Grebennikov, A. High-efficiency class E/F lumped and transmission-line power amplifiers. *IEEE Trans. Microw. Theory Tech.* **2011**, *59*, 1579–1588. [[CrossRef](#)]
- Rivas, J.M.; Han, Y.; Leitermann, O.; Sagneri, A.D.; Perreault, D.J. A High-Frequency Resonant Inverter Topology With Low-Voltage Stress. *IEEE Trans. Power Electron.* **2008**, *23*, 1759–1771. [[CrossRef](#)]
- Aldhaher, S.; Yates, D.C.; Mitcheson, P.D. Modeling and Analysis of Class EF and Class E/F Inverters With Series-Tuned Resonant Networks. *IEEE Trans. Power Electron.* **2016**, *31*, 3415–3430. [[CrossRef](#)]
- You, F.; He, S.; Tang, X.; Deng, X. High-Efficiency Single-Ended Class-EF₂ Power Amplifier With Finite DC Feed Inductor. *IEEE Trans. Microw. Theory Tech.* **2009**, *58*, 32–40.
- Grebennikov, A. Load network design techniques for class E RF and microwave amplifiers. *High Freq. Electron.* **2004**, *3*, 18–32.
- Grebennikov, A. High-efficiency class-FE tuned power amplifiers. *IEEE Trans. Circuits Syst. I Regul. Pap.* **2008**, *55*, 3284–3292. [[CrossRef](#)]

Disclaimer/Publisher’s Note: The statements, opinions and data contained in all publications are solely those of the individual author(s) and contributor(s) and not of MDPI and/or the editor(s). MDPI and/or the editor(s) disclaim responsibility for any injury to people or property resulting from any ideas, methods, instructions or products referred to in the content.